Doubly Radiative *np* Capture*

Ronald J. Adler
The American University, Washington, D.C. 20016, and
Stanford Linear Accelerator Center, Stanford University, Stanford, California 94305
(Received 24 April 1972)

We have calculated the cross section for $n+p \to d+2\gamma$. This process depends critically on the same matrix element that gives the amplitude for singly radiative *np* capture from the continuum ^3S state. It has been suggested that "anomalous" transitions from this continuum ^3S state may explain a long-standing discrepancy in *np* capture ($\sigma_{exp} = 334.2 \pm 0.5$ mb and $\sigma_{th} = 309.5 \pm 5$ mb) by contributing roughly 8% to the total *np* capture cross section. If this speculation is correct then the branching ratio of doubly to singly radiative *np* capture is 1.4×10^{-4}. On the other hand a conventional estimate of this amplitude yields a branching ratio of about 3.4×10^{-10}. An experimental measurement of the doubly radiative cross section in the 10-μb region should therefore settle the question of the importance of the ^3S initial state in the total radiative *np* capture cross section. Such a measurement seems at present to be much easier than similarly motivated polarization measurements.

I. INTRODUCTION

In previous work[1-3] it has been shown that a discrepancy of about 8% still seems to exist between theory and experiment for the process of thermal radiative neutron capture on protons. This is termed, after Austern and Rost,[4] the interaction effect. In our opinion the best values to date are 334.2 ± 0.5 mb for experiment[5] and 309.5 ± 5 mb for theory.[1] The present work was motivated by the slim possibility that the doubly radiative cross section, that is $n+p \to d+2\gamma$, might be anomalously large and thereby explain the interaction effect, since the number of capture γ rays is not in general measured in experiments. In this work we find that the doubly radiative cross section is many orders of magnitude too small to explain the interaction effect. There is however a very interesting relation between the doubly radiative cross section and the singly radiative cross section for capture from the ^3S *np* state.

To be specific we find in this work that the doubly radiative cross section depends critically on the overlap integral between the ^3S continuum wave function and the deuteron wave function. These states are normally considered to be orthogonal, and an estimate based on this assumption yields a doubly radiative cross section of only 10^{-4} μb. On the other hand, if the overlap integral is anomalously large[2,6] and roughly equal to that between the ^1S continuum wave function and the deuteron wave function, two things occur: (1) the singly radiative capture cross section from the ^3S state increases greatly, becoming about 8% of that from the ^1S state and raising the total theoretical cross section to agree with the experimental value; (2) the doubly radiative cross section increases enormously, from 10^{-4} μb to about 42 μb. The doubly radiative process thus becomes measurable.

Our understanding of nucleon dynamics is not complete so we cannot definitely rule out the possibility of an anomalously large overlap integral between the ^3S continuum wave function and deuteron wave function. An experimental measurement of the doubly radiative cross section should provide a direct test of this orthogonality and thus, indirectly, a clarification of the role of the ^3S initial state in single radiative capture.

Our calculation is based on the diagrams in Fig. 1, although we will only use Fig. 1(a). Our use of these diagrams is justified, in Sec. 2, by the position of their singularities.[7-10] The amplitude described by Fig. 1(a) involves a generalized Compton amplitude, wherein a nucleon emits two photons and becomes virtual, as shown in Fig. 2. This amplitude will be obtained in Sec. 3, in analogy with the Compton-scattering low-energy theorem of Goldberger and Gell-Mann,[11] and Low,[12] the GGL theorem. The relation between the two diagrams in Fig. 1 will be discussed in Sec. 4, and we will justify our neglect of Fig. 1(b). In Secs. 5 and 6 we will calculate the total cross section for capture from the two $l=0$ states, ^1S and ^3S, that are expected to dominate. Within conventional theory, assuming orthogonality of the ^3S and the deuteron wave functions the doubly radiative cross section is found to be of order 10^{-4} μb. If the orthogonality is sacrificed, however, we find, as noted previously, that the doubly radiative cross section could be as large as 42 μb. In Sec. 8 we summarize briefly the theory of sing-

ly radiative *np* capture,[1,2] and show the relation between singly radiative capture from the ^3S state and doubly radiative capture.

Two Appendixes are included, one in which some details of the singularity structure of several skeletonized Feynman diagrams are discussed, and another in which our calculation method in terms of wave functions is heuristically derived.

2. CHOICE OF DIAGRAMS

There are numerous diagrams one may draw to represent the interaction of two photons with a neutron-proton system and some criterion for the selection of the most important diagrams is necessary. We wish to justify the choice of the two already discussed, as drawn in Fig. 1. For this purpose we will investigate the analytic structure of the amplitudes corresponding to various diagrams. There are well known and very convenient techniques for studying the analytic structure of Feynman amplitudes without actually performing the various integrals; in particular the singularities of the amplitudes may be obtained by the methods of Landau,[7] Cutkosky,[8] and Bjorken.[9,10] We will follow the standard practice in dispersion calculations of assuming that the diagrams with singularities closest to the physical region are dominant.[10,13]

We wish to emphasize that our classification of diagrams according to their singularity structure is quite independent of the actual means of calculation.[14,15] We will in fact use a nonrelativistic reduction of the Feynman amplitudes as discussed in several previous works[1,14-16] and summarized in Appendix B.

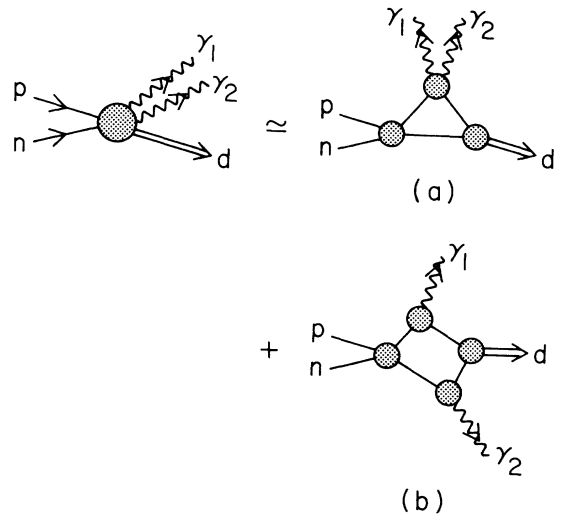

FIG. 1. The diagrams which represent the processes discussed in this paper. The first, (a), is the "Compton-like" process wherein one nucleon emits two real photons and enters the deuteron state with respect to the other nucleon, very much as in singly radiative *np* capture. The second, (b), is the "interference" process in which both nucleons emit a single photon.

Let us choose convenient variables in terms of which the amplitude may be assumed to be an analytic function with isolated singularities. We will work in a frame where the neutron and proton are both initially at rest and have zero relative momentum. The two photons then are emitted with four-momenta q_1 and q_2, while the deuteron recoils with three-momentum equal to $-(\vec{q}_1+\vec{q}_2)$. We will consider the amplitude as a function of the invariant four-vector square,

$$q^2=(q_1+q_2)^2 \tag{2.1}$$

and the angle θ between the photons, as shown in Fig. 3. The choice of q^2 is in close analogy to common practice in electron scattering theory.[10,17,18] The sum of the photon energies is equal to ϵ, the deuteron binding energy, if the deuteron recoil energy is neglected. Thus we may write the invariant q^2 approximately as

$$q^2=(q_1+q_2)^2=2q_1\cdot q_2=4|\vec{q}_1|(\epsilon-|\vec{q}_1|)\sin^2\tfrac{1}{2}\theta \tag{2.2}$$

when the emitted photons are on the mass shell, i.e., in the physical region. The physical region in q^2 is thus the region from $q^2=0$ to $q^2=\epsilon^2$ traced out as $|\vec{q}_1|$ runs from 0 to ϵ and θ runs from 0 to π. In terms of the nearest singularity in the amplitude, which we shall find is $q^2=4\epsilon M$, this is very close to the origin $q^2=0$. For simplicity in this section we will consider the special case of $q_1\cdot q_2$

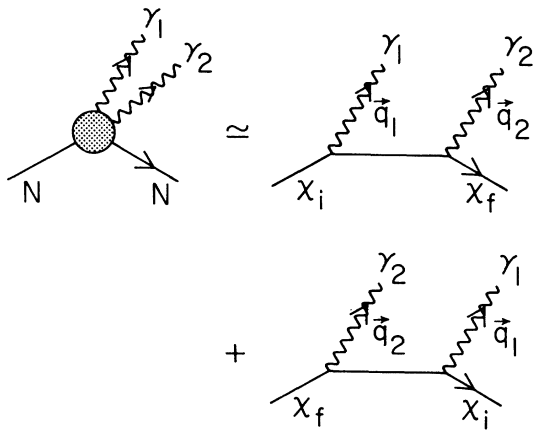

FIG. 2. The diagrammatic content of the generalized Compton amplitude used in this work. The photon γ_1 has three-momentum $\vec{q}_1$, energy ω_1, and polarization vector $\vec{\epsilon}_1$, and similarly for photon γ_2. The nucleon has an initial spin χ_i, final spin χ_f, charge e, and magnetic moment μ. We consider the nucleon to be initially at rest.

$=0$ which corresponds to $\theta=0$ in the physical region, and to $q^2=q_1^2+q_2^2$ throughout the q^2 plane.

Having chosen the convenient variable q^2 we may refer to the literature[17,18] to obtain the position of singularities in the q^2 plane. Only one unorthodox feature is involved in our analysis; as is customary, we consider the nucleons, deuteron, and photons as real external particles, but we *also* consider the continuum *np* system as a fictitious particle whose mass is equal to the sum of the neutron and proton masses. It is thus analogous to a bound *np* system in the limit of zero binding energy. This procedure is easily justified for a given diagram, and in general one may say that the position of the singularity is a continuous function of the mass of the external "particle," i.e., the continuum *np* system.[19] This is discussed further in Appendix A.

In Fig. 4 we have listed a number of skeleton diagrams contributing to doubly radiative *np* capture. The nearest singularity to the physical region $q^2\simeq 0$, is at $q^2=4M\epsilon$, which occurs for the Compton-like amplitude in Fig. 4(a) which is the same as Fig. 1(a). Figure 4(b) is merely one way in which the generalized Compton amplitude in Fig. 4(a) can be dissected and must have the same singularity position, which is easy to verify explicitly. Figure 4(c) is another way to draw Fig. 4(b) and is included as a consistency check. Figure 4(d) is the interference term that occurs also in Fig. 1(b), and also has a singularity at $q^2=4M\epsilon$. Therefore the diagrams 4(a) to 4(d) all have the same singularity position; they are clearly contained implicitly in the diagrams of Fig. 1. The remaining diagrams have singularities which are at least 5 times as far from $q^2=0$ and will be neglected. We thereby have a plausible justification for retaining only the diagrams in Fig. 1, as already discussed in the Introduction.

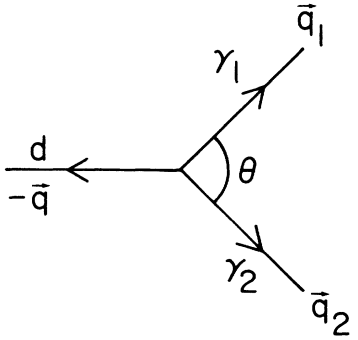

FIG. 3. Kinematics of the doubly radiative capture process. The deuteron recoils with three-momentum $(-\vec{q})$, where $\vec{q}=\vec{q}_1+\vec{q}_2$. Compared to its rest mass the kinetic energy associated with this recoil is negligible.

In Appendix A the behavior of the singularity as a function of the mass of the *np* system for Fig. 4(a) is discussed further (see Fig. 5), as well as the singularity positions of the other diagrams in Fig. 4.

3. GENERALIZED LOW-ENERGY COMPTON AMPLITUDE

Compton scattering on spin $\frac{1}{2}$ targets is a well-studied process. The expansion of the amplitude in powers of the photon energy was investigated by Gell-Mann and Goldberger,[11] and Low,[12] in 1954. They discovered that to first order in ω, the incident photon energy, the amplitude is expressible in terms of only the charge and magnetic moment of the target. Their result is derivable on such general grounds that it is generally referred to as a low-energy theorem. More recently systems of higher spin have been studied, and higher powers in ω considered; the resultant amplitudes of course contain structure-dependent functions.[20,21]

Our present concern is with photons of frequency around 1 MeV, so a low-energy theorem is pre-

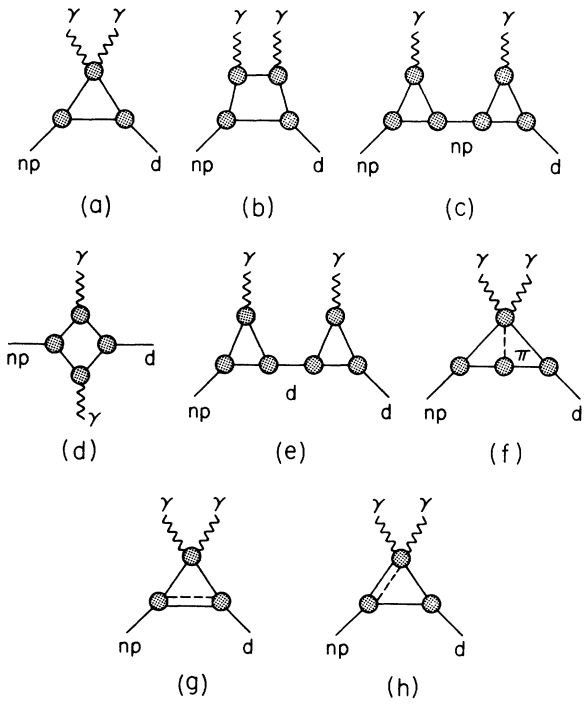

FIG. 4. Some diagrams whose singularity position is considered in Sec. 2 and Appendix A. Diagrams (a), (b), and (c) are implicitly contained in the diagram in Fig. 1(a), while (d) is the same as Fig. 1(b). These are singular at $q^2=4M\epsilon$. Other singularities are at: (e) $20M\epsilon$; (f) $4\mu^2$, where μ is the pion mass; (g) $16\mu M$; (h) $2M\mu$.

cisely what we need. We must, however, consider a situation where two photons of arbitrary frequency are emitted forward in time. The GGL theorem is obtained by either classical means, renormalized quantum field theory, or by evaluation of Feynman diagrams. We therefore expect a generalized Compton amplitude as calculated from the Feynman diagrams in Fig. 2 to be a good approximation; indeed the GGL low-energy theorem is a special case, and provides an "anchor" when one photon line is time reversed.

It is straightforward to obtain the low-energy amplitude for Fig. 2. We merely write the Dirac spinors and matrices in terms of Pauli spinors χ and spin matrices σ, and retain appropriate powers of the momenta and energy. For the np capture problem the initial neutron and proton are very nearly at rest in the lab frame so we will obtain our generalized Compton amplitude for a nucleon originally at rest.

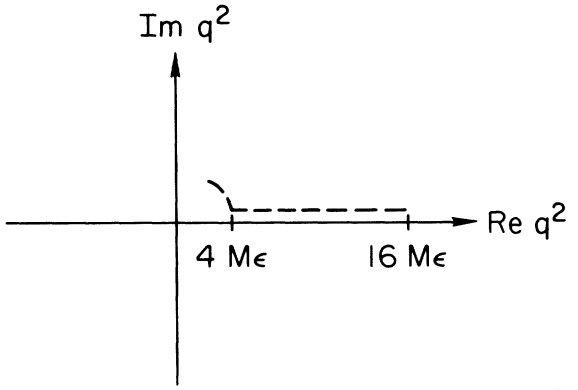

FIG. 5. Position of the singularity of Fig. 4(a). As the np mass varies from $2M-\epsilon$ to $2M$ the singularity moves along the real axis from $16M\epsilon$ to $3M\epsilon$. As the kinetic energy, κ, of the np system increases (a further mass increase) the singularity moves off axis along a parabola, as seen from Eq. (A1). The motion is continuous.

Evaluation of the diagrams in Fig. 2 yields the invariant amplitude

$$A=\frac{e^2}{(4\omega_1\omega_2)^{1/2}}\chi_f^+[T_{\mu\nu}\epsilon_1^\mu\epsilon_2^\nu]\chi_i=\frac{e^2}{(4\omega_1\omega_2)^{1/2}}\chi_f^+T\chi_i\,, \tag{3.1}$$

where the bracket corresponds to a generalized GGL Compton amplitude and is explicitly given by

$$\begin{aligned}T_p=&\frac{\vec{\epsilon}_1\cdot\vec{\epsilon}_2}{M}+\frac{(\omega_1+\omega_2)}{4M^2}\vec{\epsilon}_1\cdot\vec{\epsilon}_2+\frac{(\omega_1+\omega_2)\mu_p{}^2}{4M^2}(\vec{n}_2\times\vec{\epsilon}_2)\cdot(\vec{n}_1\times\vec{\epsilon}_1)\\&+\frac{i\mu_p{}^2(\omega_2-\omega_1)}{4M^2}(\vec{\epsilon}_2\times\vec{n}_2)\times(\vec{\epsilon}_1\times\vec{n}_1)\cdot\vec{\sigma}+\frac{i(\mu_p-1)(\omega_1-\omega_2)}{4M^2}(\vec{\epsilon}_2\times\vec{\epsilon}_1\cdot\vec{\sigma})\\&-\frac{i\mu_p}{2M^2}\left[\omega_1\vec{\sigma}\cdot\left\{\frac{\vec{n}_1(\vec{n}_1\times\vec{\epsilon}_1)+(\vec{n}_1\times\vec{\epsilon}_1)\vec{n}_1}{2}\right\}\cdot\vec{\epsilon}_2+\omega_2\vec{\sigma}\cdot\left\{\frac{\vec{n}_2(\vec{n}_2\times\vec{\epsilon}_2)+(\vec{n}_2\times\vec{\epsilon}_2)\vec{n}_2}{2}\right\}\cdot\vec{\epsilon}_1\right]\end{aligned} \tag{3.2a}$$

for the proton; only the protons charge e_p and magnetic moment μ_p enter to first order in frequency. For the neutron only the terms quadratic in the magnetic moment occur since there is no charge scattering[11]

$$T_n=\frac{(\omega_1+\omega_2)\mu_n{}^2}{4M^2}(\vec{n}_2\times\vec{\epsilon}_2)\cdot(\vec{n}_1\times\vec{\epsilon}_1)+\frac{i\mu_n{}^2(\omega_2-\omega_1)}{4M^2}(\vec{\epsilon}_2\times\vec{n}_2)\times(\vec{\epsilon}_1\times\vec{n}_1)\cdot\vec{\sigma}\,. \tag{3.2b}$$

For brevity we shall write either amplitude as

$$T=T_0+\vec{B}\cdot\vec{\sigma}\,, \tag{3.3}$$

where T_0 refers to the first three terms in (3.2a) or the first term in (3.2b) which contain no spin operators, and $\vec{B}\cdot\vec{\sigma}$ refers to the remaining terms. In analogy with low-energy Compton scattering, which we will discuss below, T_0 will be called the Thompson term and $\vec{B}\cdot\vec{\sigma}$ the spin-flip term.

As an anchor to the GGL theorem we note that for the case $\omega_1=-\omega_2=-\omega$, corresponding to Compton scattering, the amplitude (3.2a) reduces to

$$\begin{aligned}T_p=&\frac{\vec{\epsilon}_1\cdot\vec{\epsilon}_2}{M}+\frac{i\mu_p{}^2 2\omega}{4M^2}(\vec{\epsilon}_2\times\vec{n}_2)\times(\vec{\epsilon}_1\times\vec{n}_1)\cdot\vec{\sigma}\\&-\frac{i\mu_p\omega}{2M}\left[\vec{\sigma}\cdot\left\{\frac{\vec{n}_2(\vec{n}_2\times\vec{\epsilon}_2)+(\vec{n}_2\times\vec{\epsilon}_2)\vec{n}_2}{2}\right\}\cdot\vec{\epsilon}_1-\vec{\sigma}\cdot\left\{\frac{\vec{n}_1(\vec{n}_1\times\vec{\epsilon}_1)+(\vec{n}_1\times\vec{\epsilon}_1)\vec{n}_1}{2}\right\}\cdot\vec{\epsilon}_2\right]+\frac{i(\mu_p-1)2\omega}{4M^2}(\vec{\epsilon}_2\times\vec{\epsilon}_1\cdot\vec{\sigma})\end{aligned} \tag{3.4}$$

which agrees with the familiar result of GGL.[11,12]

It is clear that the process of $N \to N+2\gamma$ is kinematically forbidden for a free nucleon, N. In the problem under consideration the final nucleon is bound in the deuteron and is no longer on the mass shell, so the process becomes allowed. It should be stressed that the exact amplitude which should be used for the two-photon emission would therefore involve an off-mass-shell final nucleon. Our assumption is that the amplitude is a smooth function of the mass of the final nucleon.

4. ISOTOPICS AND THE INTERFERENCE DIAGRAM

The two diagrams in Fig. 1 are not entirely independent but may be related by isotopics if we assume that there exists an analog of the generalized low-energy Compton amplitude of Sec. 3 in a form which we will discuss. We will assume, for the same reasons as for singly radiative np capture, that the neutron is captured predominantly from the two $l=0$ states, the ^1S and ^3S.

Consider capture from the ^1S state first. This involves an isovector transition of the np system, so the general form of amplitude that results from evaluating the diagram in Fig. 1(a) can be inferred from Eqs. (3.2a) and (3.2b) to be

$$A_1 = A(e_p^2 - e_n^2) + B[e_p(e\mu_p) - e_n(e\mu_n)] + C[(e\mu_p)^2 - (e\mu_n)^2], \tag{4.1}$$

where $e_p = e$ is the proton charge and we have formally retained the neutron charge, $e_n = 0$, to make the isovector nature manifest: only *differences* between proton and neutron parameters occur. The coefficients A, B, and C will of course depend on the np wave functions and spin matrix elements; these will be discussed in the following sections but here we wish to leave them unspecified. In similar fashion we see that Fig. 1(b) will lead to an amplitude with the general form

$$A_2 = D(e_p e_n) + F[e_p(e\mu_n) - e_n(e\mu_p)] + G(e\mu_p)(e\mu_n). \tag{4.2}$$

Only products of neutron and proton parameters occur in the interference term.

We can tie together the amplitudes in (4.1) and (4.2) if we assume that, in analogy with the results of Sec. 3, the total amplitude can be obtained from the diagrams of Fig. 6. That is, the np system in the ^1S and $I=1$ state emits a photon and proceeds as either an $I=0$ or $I=1$ virtual np state, then emits another photon to emerge as an $I=0$ deuteron. Since one vertex must be isovector and the other isoscalar the general form of this amplitude is easily seen to be

$$A_3 = H(e_p - e_n)(e_p + e_n) + I(e_p - e_n)(e\mu_p + e\mu_n) + J(e\mu_p - e\mu_n)(e_p + e_n) + K(e\mu_p + e\mu_n)(e\mu_p - e\mu_n). \tag{4.3}$$

Each term is the product of an isovector and an isoscalar two-nucleon vertex function. If we now set $A_3 = A_1 + A_2$ we find that the coefficients of the nucleon charge and moment parameters must obey

$$H = A, \quad K = C, \quad D = 0, \quad G = 0, \quad B = J + I, \quad F = I - J. \tag{4.4}$$

Only F remains from Fig. 1(b). We will see in Secs. 5 and 6 that only a reasonable approximation for the ^1S initial-state amplitude is of physical interest; for simplicity we will therefore make the optimistic assumption that F does not overpower A, B, and C, so that Fig. 1(b) may be ignored. In summary, for the ^1S initial state, we have only the amplitude from Fig. 1(a) which for $e_n = 0$ has the general form

$$A_1 = Ae_p^2 + Be_p(e\mu_p) + C[(e\mu_p)^2 - (e\mu_n)^2]. \tag{4.5}$$

Consider next capture from the ^3S state. We proceed as before and write for the amplitude corresponding to Fig. 1(a)

$$A_4 = a(e_p^2 + e_n^2) + b[e_p(e\mu_p) + e_n(e\mu_n)] + c[(e\mu_p)^2(e\mu_n)^2] \tag{4.6}$$

and Fig. 1(b)

$$A_5 = d(e_p e_n) + f[e_p(e\mu_n) + e_n(e\mu_p)] + g(e\mu_p)(e\mu_n). \tag{4.7}$$

The amplitude corresponding to Fig. 6 is

$$A_6 = h(e_p + e_n)^2 + m(e_p - e_n)^2 + n(e_p + e_n)(e\mu_p + e\mu_n) + p(e_p - e_n)(e\mu_p - e\mu_n) + q(e\mu_p + e\mu_n)^2 + r(e\mu_p - e\mu_n)^2. \tag{4.8}$$

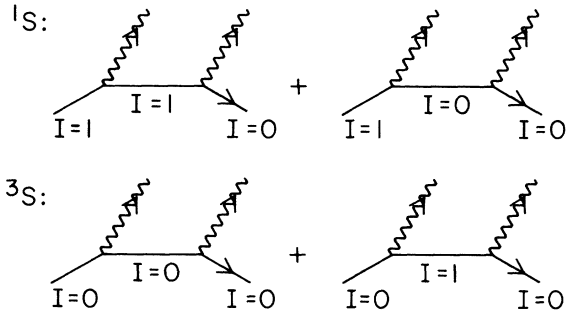

FIG. 6. Isotopics of the capture process as discussed in Sec. 4. The ^1S initial state has $I=1$, the ^3S initial has $I=0$. The $\Delta I=0$ vertices involve isoscalar nucleon parameters and the $\Delta I=1$ involve isovector parameters.

Now equating $A_6 = A_4 + A_5$ we obtain

$$a = h + m, \quad d = 2(h - m), \quad c = q + r, \quad b = n + p,$$
$$f = n - p, \quad g = 2(q - r). \tag{4.9}$$

As we will show in Sec. 6, b and c are small compared to a. Thus (4.9) leads us to expect that, since there are no selection rules forbidding either $I=0$ or $I=1$ intermediate states, a and d are large while $b, c, f,$ and g are small. This implies, as we will see in more detail in Sec. 6, that amplitude for capture from the ^3S state takes the form, with $e_n = 0$,

$$A_4 = a e_p^2. \tag{4.10}$$

We conclude that with our assumptions and within the approximations discussed we can neglect the amplitude corresponding to Fig. 1(b) for both the ^1S and ^3S initial states.

5. ^1S INITIAL STATE

We wish to show in this section that the cross section for doubly radiative np capture from the ^1S initial state alone is extremely small. The discussion of the preceding sections and Eqs. (3.2a) and (3.2b) provides us with the means of calculating the amplitude corresponding to Fig. 1(a). Indeed as has been extensively discussed in the literature the S matrix may be written as a three-dimensional matrix element of an appropriate amplitude, that is the generalized Compton amplitude, between the initial state ϕ_i and the final state ϕ_f of the np system, with momentum conservation, phase, and normalization factors.[1, 14-16] A very simple and heuristic derivation of this result, based on Feynman diagrams, is also given in Appendix B.[14-16] In terms of generalized Compton amplitudes T of Sec. 4 we therefore write

$$S = ie^2(2\pi)^4\delta^4(Q' - Q + q)(4\omega_1\omega_2)^{-1/2} \times \int \phi_f^\dagger(y) T^{(A)} \phi_i(y) e^{-i\vec{y}\cdot\vec{q}/2} d^3y, \tag{5.1}$$

where Q is the initial np total four-momentum, Q' is the final deuteron four-momentum, q is the total four-momentum of both photons, and $T^{(A)}$ will be further discussed below.

We noted in the preceding section that thermal np capture should be dominantly from the $l=0$ states, ^1S and ^3S. The ^1S state is an $I=1$ state whereas the deuteron is $I=0$. Thus, as discussed in Sec. 4 and written in (4.1), capture from the ^1S state involves only the difference between proton and neutron amplitudes. The $T^{(A)}$ amplitude in (5.1) should therefore be the difference between the proton and neutron generalized Compton amplitudes as obtained in (3.2a) and (3.2b). In the next section when we discuss the ^3S state with $I=1$ we will use a similar expression, but with $T^{(A)}$ equal to the sum of proton and neutron generalized Compton amplitudes.

For the deuteron and continuum np wave functions we use the following standard forms:

$$\phi_i(y) = (4\pi)^{-1/2}[z(y)/y]\chi,$$
$$\phi_f(y) = (4\pi)^{-1/2}\left[\frac{u(y)}{y} + \frac{w(y)}{\sqrt{8}\,y} S_{12}(\hat{y})\right]\chi_m; \quad \hat{y} = \vec{y}/|\vec{y}|. \tag{5.2}$$

The functions z, u, and w represent the zero-energy continuum np wave function, the S-wave component of the deuteron wave function, and the D-wave component of the deuteron wave function; S_{12} is the well-known tensor operator of nuclear physics and χ_m is the deuteron two-nucleon Pauli spin function given by

$$\chi_{+1} = \alpha\alpha, \quad \chi_0 = (\alpha\beta + \beta\alpha)/\sqrt{2}, \quad \chi_{-1} = \beta\beta. \tag{5.3}$$

The first spinor represents the proton spin state and the second, the neutron spin state. The spin function χ_s for the initial np continuum state will be

$$\chi_s = (\alpha\beta - \beta\alpha)/\sqrt{2} \tag{5.4}$$

for the ^1S or singlet state, and the same as in (5.3) for the ^3S or triplet state. We will use a subscript "s" or "t" on the function z to distinguish between singlet and triplet states.

Evaluation of (5.1) is elementary. We first note that $|\vec{q}|$ is of order $\epsilon \sim 2$ MeV, or ~ 0.01 fm^{-1} in natural units, while $y \lesssim 4$ fm. Thus $\vec{q}\cdot\vec{y}$ is of order 4×10^{-2}. We may therefore replace the exponential in (5.1) by unity. It is then quite easy to evaluate (5.1) by substituting the isovector amplitude $T^{(A)}$ from (3.2a) and (3.2b). Since the generalized Compton amplitude T is independent of y, one easily verifies that the D state of the deuteron wave function drops out of (5.1) by orthogonality of the angular wave functions. Moreover, the first term of T, the Thompson term T_0 as written in (3.3), does not contribute due to the orthogonality of the triplet and singlet spin functions. What remains is the product of the spin-flip term of the generalized Compton amplitude and an overlap of the functions z_s and u, with appropriate phase, normalization, and momentum-conservation factors. Specifically, after substitution (5.1) reduces to

$$S = ie^2(2\pi)^4\delta^4(Q' - Q + q)\frac{1}{(4\omega_1\omega_2)^{1/2}}(\chi_m^\dagger \vec{\sigma}_p \cdot \vec{B}\chi_s)H_s, \tag{5.5}$$

where H_s is the same overlap integral that appears in single radiative np capture

$$H_s = \int_0^\infty u(y) z_s(y) dy \tag{5.6}$$

and $\vec{B}$ is the coefficient of σ in the amplitude $T^{(A)}$ for the isovector transition, as written in (3.3):

$$\vec{B}=\frac{i}{4M^2}\{(\mu_p^2-\mu_n^2)(\omega_2-\omega_1)(\vec{\epsilon}_2\times\vec{n}_2)\times(\vec{\epsilon}_1\times\vec{n}_1)-(\mu_p-1)(\omega_2-\omega_1)(\vec{\epsilon}_2\times\vec{\epsilon}_1)$$
$$-\omega_1\mu_p[\vec{n}_1(\vec{n}_1\times\vec{\epsilon}_1)+(\vec{n}_1\times\vec{\epsilon}_1)\vec{n}_1]\cdot\vec{\epsilon}_2-\omega_2\mu_p[\vec{n}_2(\vec{n}_2\times\vec{\epsilon}_2)+(\vec{n}_2\times\vec{\epsilon}_2)\vec{n}_2]\cdot\vec{\epsilon}_1\}. \tag{5.7}$$

It is now only necessary to do phase-space integration and spin sums on the S matrix (5.5) to obtain a cross section for the ^1S initial state. This is quite simple and the result is a doubly differential cross section

$$\frac{d\sigma_s}{d\Omega\, d(\omega_2-\omega_1)}=\frac{4\pi e^4[\epsilon^2-(\omega_2-\omega_1)^2]}{32(2\pi)^5 v_n}\left(\frac{H_s^2}{4}\right)|\vec{B}^2|, \tag{5.8}$$

where v_n is the incident neutron velocity. This is easily integrated and a total cross section obtained

$$\sigma_s(2\gamma)=\sigma(1\gamma)\left(\frac{e^2}{4\pi}\right)\left(\frac{\epsilon}{M}\right)^2\left(\frac{1}{75\pi}\right)\left[(\mu_p+\mu_n)^2+\frac{4\mu_p^2-2\mu_p+1}{(\mu_p-\mu_n)^2}\right]. \tag{5.9}$$

Here $\sigma(1\gamma)$ is an approximation to the singly radiative theoretical cross section, given by[1]

$$\sigma(1\gamma)=\frac{e^2\epsilon^3 H_s^2(\mu_p-\mu_n)^2}{(4\pi)4M^2 v_n}\simeq 300\text{ mb}. \tag{5.10}$$

Note that due to the configuration space independence of the spin-flip term of the generalized Compton amplitudes (3.2) the total cross section (5.9) depends on the *np* wave functions only through the simple matrix element H_s, which is the same as that which occurs in singly radiative *np* capture.[1,2] Indeed the expression $\sigma(1\gamma)$ in (5.10) accounts rather well, to about 10%, for the entire *np* radiative cross section, as we will discuss in Sec. 7. This implies in turn that the branching ratio $\sigma_s(2\gamma)/\sigma(1\gamma)$ is roughly independent of the deuteron wave functions and is given approximately by the coefficient of $\sigma(1\gamma)$ in (5.9). Numerically this is about 3.4×10^{-10}, which implies a total doubly radiative cross section of only about 10^{-4} μb for the ^1S initial state. In the context of present day experimental techniques this is probably unmeasurably small, and certainly is a negligible part of the total radiative *np* capture cross section.[1,5]

6. ^3S INITIAL STATE

In the preceding section we saw that the ^1S initial state gives rise to a very small doubly radiative capture cross section, $\sim10^{-4}$ μb. In this section we will show that the same is expected to be true of the ^3S initial state. However, this conclusion is critically dependent on the orthogonality of the ^3S continuum and the deuteron ^3S state.[2,6] If this orthogonality is not assumed we obtain a significantly larger effect, which will be discussed at the end of this section and further in Sec. 7.

Evaluation of the S matrix for Fig. 1(a) with the ^3S initial state proceeds exactly as with the ^1S initial state, with $T^{(A)}$ now equal to the *sum* of the amplitudes (3.2a) and (3.2b). Repeating the steps discussed in Sec. 5 one finds that the contributions of the spin-flip terms of the generalized Compton amplitudes are all smaller by a factor ϵ/M than the contributions of the Thompson terms. We therefore retain only the largest of the Thompson terms and discard the spin-flip terms entirely, to obtain an approximate S matrix given by

$$S=ie^2(2\pi)^4\delta^4(Q'-Q+q)(4\omega_1\omega_2)^{-1/2}$$
$$\times(\vec{\epsilon}_1\cdot\vec{\epsilon}_2/M)\left[\int_0^\infty u(y)z_t(y)\,j_0\left(\frac{qy}{2}\right)dy(\chi_m^\dagger\chi_{m'})-\frac{1}{\sqrt{8}}\int_0^\infty w(y)z_t(y)\,j_2\left(\frac{qy}{2}\right)dy(\chi_m^\dagger S_{12}(\hat{q})\chi_{m'})\right];\quad \hat{q}=\vec{q}/|\vec{q}| \tag{6.1}$$

which represents both photons being emitted by the proton via a Thompson-like amplitude. The j_0 and j_2 which occur in (6.1) are spherical Bessel functions.

The integrals over the deuteron wave functions that occur in (6.1) also occur in the theory of inelastic electron-deuteron scattering[18] and in the theory of singly radiative *np* capture.[1,2] They are referred to as H_t and J_t. In terms of H_t and J_t the S matrix is

$$S=ie^2(2\pi)^4\delta^4(Q'-Q+q)(4\omega_1\omega_2)^{-1/2}(\vec{\epsilon}_1\cdot\vec{\epsilon}_2/M)[H_t\chi_m^\dagger\chi_{m'}-J_t\chi_m^\dagger S_{12}(\hat{q})\chi_{m'}]. \tag{6.2}$$

The sum over spins and phase-space integration is elementary, as before, and yields a doubly differential cross section given by

$$\frac{d\sigma_t}{d\Omega\, d(\omega_2-\omega_1)}=\frac{4\pi e^4[e^2-(\omega_2-\omega_1)^2]}{(2\pi)^5 v_n 32}\times\frac{3(H_t^2+8J_t^2)}{4M^2}(1+\cos^2\theta)\,. \tag{6.3}$$

The total cross section is obtained by simple integration

$$\sigma_t(2\gamma)=\sigma(1\gamma)(e^2/4\pi)\frac{4(H_t^2+8J_t^2)}{3\pi(\mu_p-\mu_n)^2H_s^2}\,, \tag{6.4}$$

where $\sigma(1\gamma)=300$ mb is the singly radiative cross section in (5.10), and H_s is the same matrix element as in (5.6).

Let us consider the matrix elements that occur in the result (6.4) and make an approximate evaluation. For this purpose we may use the well-known zero-range approximations to the various np wave functions. Consider first H_s. The zero-range wave functions for u and z_s are,

$$u(y)=\sqrt{2\alpha}\,e^{-\alpha y};\quad \alpha=\sqrt{\epsilon M};\qquad z_s(y)=\sqrt{4\pi}\,(y-a_s);\quad a_s=\text{singlet scattering length} \tag{6.5}$$

so that

$$H_s=\sqrt{4\pi}\,\sqrt{2\alpha}\left(\frac{1-\alpha a_s}{\alpha^2}\right). \tag{6.6}$$

The matrix element J_t involves the spherical Bessel function $j_2(qy/2)$. Since the argument is very small we expand and retain only the lowest-order term in $q=\epsilon$, which implies that $j_2=0(\epsilon^2y^2)$ and

$$J_t\cong\frac{\epsilon^2}{60\sqrt{8}}\int_0^\infty w(y)z_t(y)y^2dy\,. \tag{6.7}$$

To evaluate this we shall use the zero-range continuum state

$$z_t(y)=\sqrt{4\pi}\,(y-a_t);\quad a_t=\text{triplet scattering length}\,. \tag{6.8}$$

For the deuteron D wave a rather crude tail approximation will be used

$$w(y)=\eta\sqrt{2\alpha}\,e^{-\alpha y}. \tag{6.9}$$

Here η is the asymptotic D to S ratio of the deuteron, numerically[22] about 3×10^{-2}. This approximation for $w(y)$ is justified by the factor y^2 in (6.7) that weights the large y region where (6.9) is a decent approximation at the expense of the small y region, where it is not. The result is

$$J_t\cong\frac{\epsilon^2}{60\sqrt{8}}\left[\frac{2\sqrt{4\pi}\,\sqrt{2\alpha}\,\eta}{\alpha^3}\left(\frac{3}{\alpha}-a_t\right)\right]\cong\sqrt{4\pi}\,\sqrt{2\alpha}\left(\frac{\eta}{15\sqrt{8}M^2}\right), \tag{6.10}$$

where we have used the approximate relation $a_t\simeq1/\alpha$ in the last step.[23] It is evident that J_t is very much less than H_s. As we shall discuss shortly it may be totally neglected.

Finally we must consider H_t. We expand $j_0(qy/2)$ about $q=\epsilon=0$, as with $j_2(qy/2)$ above, but retain the first two terms, of order 1 and of order ϵ^2y^2:

$$H_t=\int_0^\infty u(y)z_t(y)dy-\frac{\epsilon^2}{24}\int_0^\infty u(y)z_t(y)y^2dy\,. \tag{6.11}$$

The first term is normally assumed to be zero since $u(y)$ and $z_t(y)$ are both triplet states but have different energies. In a Schrödinger theory they would therefore be orthogonal. This would also be true in any theory where the two-nucleon dynamics are determined by a unitary time-displacement operator, i.e., where the two-nucleon Hamiltonian is Hermitian. It has been speculated, however, that a lack of orthogonality is possible since our understanding of two-nucleon dynamics is incomplete. Moreover, such a nonorthogonality might solve the problem of the interaction effect.[1-6] We will return to this question later in Sec. 7. For now we will merely set the first term in (6.11) equal to H_s times a dimensionless parameter Λ. Orthogonality then corresponds to $\Lambda=0$.

The second term of (6.11) is easily obtained using the wave functions (6.5) and (6.8), so H_t may be written as

$$H_t=\Lambda H_s-\sqrt{4\pi}\,\sqrt{2\alpha}\left(\frac{1}{6M^2}\right), \tag{6.12}$$

where we have again used $a_t\simeq1/\alpha$. It should be noted that in the zero-range limit the wave functions u and z_t are indeed orthogonal if the above approximate triplet scattering length, $1/\alpha$, is used.

We may now substitute (6.6), (6.10), and (6.12) into (6.4) to obtain a useful form for σ_t:

$$\sigma_t(2\gamma)=\sigma(1\gamma)\frac{4}{3\pi(\mu_p^2-\mu_n^2)}\left[\Lambda-\frac{\epsilon}{6M(1-\alpha a_s)}\right]^2. \tag{6.13}$$

In (6.13) the contribution of J_t^2 has been neglected since it is ~10^3 times smaller than H_t. That is (6.13) is a pure S-wave zero-range approximation.

Equation (6.13) is the main result of this work. If the deuteron wave function u and the np continu-

um wave function z_t are orthogonal then $\Lambda = 0$ and we have, with $\epsilon = 2.22$ MeV, $\alpha = 0.232$ fm^{-1}, and $a_s = -23.7$ fm,

$$\sigma_t(2\gamma) = \sigma(1\gamma)\left(\frac{e^2}{4\pi}\right)\frac{(\epsilon/M)^2}{27\pi(\mu_p-\mu_n)^2(1-\alpha a_s)^2} = 1.6\times10^{-7}\ \mu\text{b} \tag{6.14}$$

which is quite negligible compared even to $\sigma_s(2\gamma) = 10^{-4}$ μb discussed in Sec. 5. On the other hand, Λ could be nonzero as discussed by Breit and Rustgi.[6] Indeed if $\Lambda \cong 1$ the discrepancy in the total np capture cross section disappears, as has been shown in Ref. 2, and which will be discussed in Sec. 7. For $\Lambda \cong 1$ we have from (6.13)

$$\sigma_t(2\gamma) = \sigma(1\gamma)\left(\frac{e^2}{4\pi}\right)\frac{4\Lambda^2}{3\pi(\mu_p^2-\mu_n^2)} = 42\ \mu\text{b}. \tag{6.15}$$

It is therefore clear that σ_t is quite sensitive to the orthogonality of u and z_t.

From the preceding paragraph it is clear that a measurement of the doubly radiative np capture cross section, $\sigma_s + \sigma_t$, would provide a very sensitive test of the orthogonality of the deuteron wave function u and the np continuum wave function z_t. In particular the value $\Lambda \cong 1$, which would solve the long-standing problem of the interaction effect,[6] provides a measurable cross section of about 42 μb, whereas $\Lambda = 0$ leads to the very small cross section of Sec. 5, about 10^{-4} μb.

7. RELATION TO SINGLY RADIATIVE CAPTURE

Singly radiative np capture is a well studied process and much material appears in the literature.[1-6] Here we will first summarize very briefly the results of previous work; specifically we will quote mainly from Refs. 1 and 2.

The most recent experimental result for the total thermal np capture cross section is

$$\sigma_{\text{exp}} = 334.2 \pm 0.5 \text{ mb} \tag{7.1}$$

as obtained by Cox, Wynchank, and Collie.[5] This result is in agreement with previous experimental[1] work, although more accurate, and no definite sources of systematic error have been suggested.

The theoretical treatment of the problem has been under development for many years. Calculations of the transition from the ^1S state have been made using both a nonrelativistic wave-function approach[1,3] and a dispersion theoretic approach.[24-26] We believe that these are now in substantial agreement as discussed in Ref. 1. Such small effects as meson exchange currents,[1] incoherent nucleon excitations,[27] and relativistic corrections[1,2] have been included. The result of this work, in the notation of Refs. 1 and 2 is a total cross section for capture from the ^1S state of

$$\sigma(1\gamma) = \left(\frac{e^2}{4\pi}\right)\frac{\epsilon^3(G_{12})^2}{2M^2 v_n} = 309.5 \pm 5 \text{ mb} \tag{7.2}$$

which is about 8% below the experimental value in (7.1). [The numerical value of σ in (7.2) is the conclusion of the present author and Ref. 1.]

By far the largest part of the above theoretical result is due to an impulse-approximation diagram – basically Fig. 1(a) but with a single photon emitted. The contribution of this diagram is that which is used in Secs. 5 and 6, as given in (5.10). This corresponds to an invariant amplitude G_{12} given by

$$G_{12} = \tfrac{1}{2}(\mu_p - \mu_n)H_s, \tag{7.3}$$

where H is the overlap integral between deuteron and the ^1S state already discussed in Sec. 5 and given in (5.6).

The discrepancy between experiment and theory, (7.1) versus (7.2), has stimulated interest in numerous possible mechanisms for increasing the theoretical result (7.2). In addition to the mesonic effects and relativistic corrections mentioned above it has been suggested by Breit and Rustgi[6] that transitions from the ^3S state could be anomalously large and contribute the missing 8%. Again in the notation of Ref. 2 the cross section for singly radiative capture from the ^3S state may be written

$$\sigma = \left(\frac{e^2}{4\pi}\right)\frac{\epsilon^3(G_3^2 + G_4^2)}{2M^3 v_n}. \tag{7.4}$$

Theoretical estimates of G_3 and G_4 indicate that this process is smaller than the ^1S process by about 3 orders of magnitude. This conclusion, however, is based on the orthogonality of the deuteron and ^3S states. Indeed if we ignore the D state of the deuteron we can write explicitly[2]

$$G_4 = 0, \qquad G_3 = 1/\sqrt{2}\,(\mu_p + \mu_n)H_t, \tag{7.5}$$

where H_t was discussed in Sec. 6 and is explicitly given by

$$H_t = \frac{1}{\sqrt{8}}\int_0^\infty u(y)z_t(y)\,j_0\left(\frac{qy}{2}\right)dy \simeq \Lambda H_s - \sqrt{4\pi}\,\sqrt{2\alpha}\left(\frac{1}{6M^2}\right). \tag{7.6}$$

In any theory based on a Hermitian Hamiltonian one of course expects the overlap integral to be zero, or $\Lambda = 0$. However, it is possible to question the basic interpretation of u and z_t as simple eigenvectors of a nonrelativistic theory. In a relativistic theory of strong interactions one has virtual states possible that certainly do not correspond to any nonrelativistic limit; for example,

there should be virtual mesons and virtual excited nucleon states present. It is not entirely clear how these virtual states should be treated in the nonrelativistic limit, and therefore whether the Hamiltonian describing the time evolution of the dressed two-nucleon state should indeed be strictly Hermitian.

Motivated by this uncertainty we may entertain the possibility that H_t is indeed large enough to explain the 8% discrepancy quoted above. That is we assume

$$\sigma_{\text{exp}} \cong \left(\frac{e^2}{4\pi}\right) \frac{\epsilon^3}{2Mv_n} (G_{12}^2 + G_3^2) \tag{7.7}$$

or

$$334.2 \text{ mb} = 309.5 \text{ mb} \left(1 + \frac{G_3^2}{G_{12}^2}\right),$$

$$\frac{G_3^2}{G_{12}^2} \equiv R_3^2 \cong 0.08 . \tag{7.8}$$

Then H_t is easily obtained in terms of H_s:

$$G_3 = R_3 G_{12}; \quad H_t = \frac{R_3}{\sqrt{2}} \left(\frac{\mu_p - \mu_n}{\mu_p + \mu_n}\right) H_s . \tag{7.9}$$

Thus

$$\Lambda = \frac{R_3}{\sqrt{2}} \left(\frac{\mu_p - \mu_n}{\mu_p + \mu_n}\right) = 1.06 . \tag{7.10}$$

In this estimate we have ignored the small exchange-current contribution mentioned above. The value $\Lambda \cong 1$ in (7.10) implies that the breaking of orthogonality between u and z_t is very large indeed, in that the overlap integral between u and z_t is roughly equal to that between u and z_s where no orthogonality at all is present. It appears from (7.10) and the results of Sec. 6 that a measurement of the doubly radiative np capture cross section to an accuracy about 0.01 mb should clarify the role of the ^3S state in singly radiative np capture by providing a test of u and z_t orthogonality.

Breit and Rustgi[6] have suggested that the overlap integral between u and z_t could also be measured in an experiment with polarized neutrons captured on polarized protons. The present author has analyzed this problem in more detail with qualitatively the same conclusion as Breit and Rustgi.[2] Such an experiment, where one measures the angular distribution of the γ rays emitted in the capture process, however, appears a great deal more difficult than a measurement of the total doubly radiative cross section to about 10 μb as discussed above.

8. CONCLUSIONS

We have estimated the doubly radiative np capture cross section to be about 10^{-4} μb, if, as is normally assumed, the deuteron ground state and the zero-energy triplet np state are orthogonal. Conversely if these states are not orthogonal, and the overlap is large enough to explain the radiative capture discrepancy, the cross section could be very much larger, about 42 μb. A measurement of this cross section should therefore be a simple way to ascertain the role of the ^3S initial state in the total np capture cross section.

APPENDIX A. SINGULARITY POSITIONS FOR SOME DIAGRAMS

We have noted in the text the singularity structure of the diagrams in Fig. 4. Several further comments are in order concerning the position of singularities. The singularity for Fig. 1(a) in the related process of elastic ed scattering is at $16\epsilon M$, which one may consider the prototype of anomalous thresholds. For our present problem we vary the mass of the external np system from $2M - \epsilon$, the deuteron mass, to $2M$, the zero-energy np mass. As we do this the singularity moves continuously from $16\epsilon M$ to $4\epsilon M$. One can verify this with the convenient geometrical method discussed by Bjorken and Drell[10] or the standard algebraic method discussed, for example, by Squires.[19] For a mass for the np system that is slightly above $2M$ we must use the algebraic method. Then if $2M + K$ is the mass the singularity moves off the real axis to a point (see Fig. 5)

$$q^2 = 4M(\epsilon - K) + 8M\sqrt{\epsilon K}\, i . \tag{A1}$$

Thus for $K \ll \epsilon$ we can ignore K to an excellent approximation and are fully justified in considering the np state as the limit of a zero-energy bound system, or "particle." Capture of thermal neutrons with 1/40 eV certainly satisfies the above energy criteria.

Having satisfied ourselves of this we can obtain the singularities of Figs. 4(c) and 4(e) in terms of the individual q_1^2 and q_2^2 singularities, since $q^2 = q_1^2 + q_2^2$ in our special case. Thus using Refs. 19 and 10 and reasoning as above we may show that for Fig. 4(c) the singularity is at $4M\epsilon$, and for Fig. 4(e) at $4M\epsilon + 16M\epsilon = 20M\epsilon$.

Diagrams 4(b) and 4(d) are conveniently handled by the geometrical method,[18] and have the same singularity as 4(a), that is, $q^2 = 4M\epsilon$. The remaining diagrams with pions are relatively insensitive to the external mass of the np system, and the position of their singularities is approximately the same as for elastic ed scattering, a well-known case. These may be obtained geometrically[10] with ease, and are given in Fig. 4.

APPENDIX B. FEYNMAN DIAGRAM AND WAVE FUNCTIONS

We wish to consider the first diagram in Fig. 1 where one of the nucleons spontaneously emits two photons and drops into the deuteron ground state with respect to the other nucleon. The amplitude for the emission of two photons by the nucleon was discussed in Sec. 3. Here we wish to justify in a simple and heuristic way the writing of the total amplitude as a simple nonrelativistic matrix element, (5.1), which arises naturally and intuitively from an approximate evaluation of the first Feynman diagram in Fig. 1. The end result is very similar to that obtained for related processes such as singly radiative capture. Our development is heuristic and follows similar work by Gross,[14] and by Kaschluhn and Lewin.[16] We include it here for completeness and because the present method is easily generalized to various other diagrams.

Let us consider the Feynman diagram in Fig. 1(a), which we have redrawn in Fig. 7 with momenta labeled. The two photons are represented by a single line of momentum q which is the sum of the photon four-momenta. The final deuteron has $Q'^2 = M_D^2$, while the initial line represents an np system of invariant mass near $2M$. By conventional diagrammatic techniques[10] the amplitude will be given by an integral of the form

$$S = \int \frac{d^4k_1 d^4k_2 d^4k_3 N}{(k_1^2 - M^2 - i\epsilon)(k_2^2 - M^2 - i\epsilon)(k_3^2 - M^2 - i\epsilon)} [\delta^4(k_1 + k_2 - Q)\delta^4(k_1 + k_3 - Q')\delta^4(k_2 - k_3 - q^3)] . \tag{B1}$$

All of the vertex functions and photon and nucleon spins are contained in the numerator function N.

Integration over the variables k_2 and k_3 is immediate. Instead of k_1 we introduce a new variable of integration λ which is the relative np four-momentum and obeys:

$$\begin{aligned} k_1 &= Q/2 + \lambda , \quad k_1 = Q'/2 + \lambda' , \\ k_2 &= Q/2 - \lambda , \quad k_3 = Q'/2 - \lambda' . \end{aligned} \tag{B2}$$

Here $\lambda' = \lambda + q/2$ and $q = Q - Q'$. Then the propagator functions become

$$\begin{aligned} k_1^2 - M^2 - i\epsilon &= \lambda^2 + \lambda \cdot Q - \beta^2 - i\epsilon , \\ k_2^2 - M^2 - i\epsilon &= \lambda^2 - \lambda \cdot Q - \beta^2 - i\epsilon , \\ k_3^2 - M^2 - i\epsilon &= \lambda'^2 - \lambda' \cdot Q - \alpha^2 - i\epsilon , \end{aligned} \tag{B3}$$

where the vectors are all four-vectors, and

$$\begin{aligned} \alpha^2 &= M^2 - \frac{M_D^2}{4} \simeq M\epsilon , \\ \beta^2 &= M^2 - \frac{Q^2}{4} \cong 0 , \end{aligned} \tag{B4}$$

for the "zero" energy np state "decaying" to a deuteron. The integrand in (B1) has six singularities in λ_0 located at position R, given approximately by

$$\begin{aligned} R_{1+} &= \frac{\vec{\lambda}^2 + \beta^2 + \vec{\lambda} \cdot \vec{Q}}{2M} + i\epsilon , \quad & R_{1-} &= -2M - i\epsilon ; \\ R_{2+} &= 2M + i\epsilon , & R_{2-} &= -\left(\frac{\vec{\lambda}^2 + \beta^2 - \vec{\lambda} \cdot \vec{Q}}{2M} \right) - i\epsilon ; \\ R_{3+} &= 2M + q_0/2 + i\epsilon , & R_{3-} &= -\left(\frac{\vec{\lambda}'^2 + \beta^2 - \vec{\lambda}' \cdot \vec{Q}'}{2M} \right) + \frac{q_0}{2} - i\epsilon . \end{aligned} \tag{B5}$$

These are shown in Fig. 7. The amplitude can thus be written as

$$S = (2\pi)^4 \delta^4(Q' - Q + q) \int \frac{d^4\lambda \, d^4\lambda'}{(2\pi)^4} \delta^4(\lambda' - \lambda - q/2) N \times [(\lambda_0 - R_{1+})(\lambda_0 - R_{1-})(\lambda_0 - R_{2+})(\lambda_0 - R_{2-})(\lambda_0 - R_{3+})(\lambda_0 - R_{3-})]^{-1} . \tag{B6}$$

This can be easily evaluated by residues using the contour C in Fig. 8.

Consider first the R_{1+} singularities alone. This contributes

$$S = i(2\pi)^4 \delta^4(Q' - Q + q) \int \frac{d^3\lambda}{(2\pi)^3} \frac{d^3\lambda'}{(2\pi)^3} (2\pi)^3 \delta^3(\lambda' - \lambda - q/2) \frac{N}{8M} \left(\frac{1}{\vec{\lambda}^2 + \beta^2} \right) \left(\frac{1}{\vec{\lambda}'^2 + \alpha^2} \right) . \tag{B7}$$

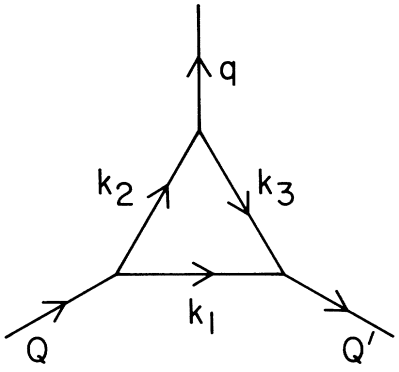

FIG. 7. The Feynman diagram discussed in Appendix B. The line labeled q here refers to the 2γ system, but the diagram and discussion are actually much more general.

We will not bother to write the contributions from the residues at R_{1+} and R_{3+}; we merely note that they involve a factor of $1/M^3$ and are therefore down by factors of p^2/M^2 from (B7), where p^2 is some characteristic energy or momentum of the problem. This is expected to be the binding energy $p \sim \epsilon \sim 2$ MeV or the wave-function momentum spread $p \sim 100$ MeV/c. In either case $p^2/M^2 \leq 10^{-2}$, so R_{1+} is by far the most important singularity.

It is easy to understand the physical significance of these results: The singularity at R_{1+} is for λ_0 very small and corresponds to the virtual nucleons being very near the mass shell, that is $k_1^0 \simeq k_2^0 \simeq k_3^0 \simeq M$. On the other hand, the singularities at R_{2+} and R_{3+} correspond to roughly $k_1^0 \simeq 3M$ and $k_2^0 \simeq k_3^0 \simeq -M$, so the nucleons are quite far off the mass shell. Clearly then the singularity at R_{1+} is the only one we need include if we intend a nonrelativistic analysis. The relative size and the meaning of the R_{2+} and R_{3+} singularities simply place them outside the scope of nonrelativistic theory. We will therefore refer to R_{1+} as the wave-function singularity.

To complete our reduction to a nonrelativistic matrix element we proceed with (B7). Note first that the factor

$$\frac{1}{\vec{\lambda}'^2+\alpha^2}=\frac{1}{4\pi}\int d^3r\,\frac{e^{-\alpha r}}{r}e^{i\vec{\lambda}'\cdot\vec{r}} \tag{B8}$$

is the Fourier transform of the asymptotic deuteron wave function $(e^{-\alpha r}/r)$. We may therefore replace the symbol $(\vec{\lambda}'^2+\alpha^2)^{-1}$ by $\phi_f^*(\lambda')$, representing the momentum-space nonrelativistic deuteron wave function.

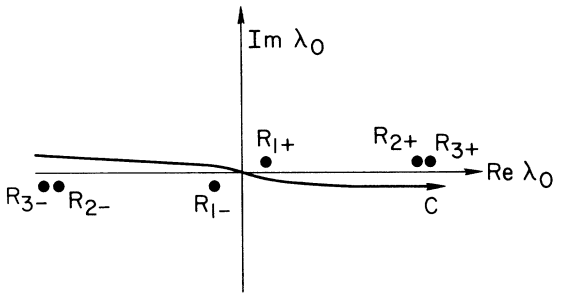

FIG. 8. The singularities in the complex λ_0 plane associated with the Feynman diagram in Fig. 7. The pole at R_{1+} is referred to as the "wave-function" pole, as discussed in Appendix B.

For the factor $(\lambda^2+\beta^2)^{-1}$ we will have similarly $\beta=0$ for a zero-energy np state, or β equal to a small imaginary number for a small relative np energy K: $\beta=i\sqrt{MK}$. As above we write

$$\frac{1}{\vec{\lambda}^2+\vec{\beta}^2}=\frac{1}{4\pi}\int d^3r\,\frac{e^{-\beta r}}{r}e^{i\vec{\lambda}\cdot\vec{r}}$$

$$=\frac{1}{4\pi}\int d^3r\,\phi_i(\vec{r})e^{i\vec{\lambda}\cdot\vec{r}}=\phi_i(\lambda)\,. \tag{B9}$$

It is now clear that S can be written as a nonrelativistic matrix element

$$S=i(2\pi)^4\delta^4(Q'-Q+q)\int\phi_f^*(\lambda+q/2)\frac{N}{8M}\phi_i(\lambda)\frac{d^3\lambda}{(2\pi)^3}\,. \tag{B10}$$

Thus our goal has been achieved. Equation (B10) represents a nonrelativistic reduction of the Feynman amplitude, and is expressed in terms of the deuteron asymptotic wave functions in momentum space and a vertex and current function. Moreover, it is very easy to see how (B10) can be generalized to more sophisticated wave functions; we merely alter ϕ_f and ϕ_i to whatever we choose, corresponding to the use of a more general or sophisticated npd vertex function. For further convenience we insert the Fourier transform of the momentum-space wave functions into (B10) and work in configuration space. The various factors in N appropriate to the nonrelativistic matrix element are quite easily guessed. We thereby arrive at a working expression for the amplitude S:

$$S=ie^2(2\pi)^4\delta^4(Q'-Q+q)\int\phi_f^*(\vec{r})A\,\phi_i(\vec{r})e^{-i\vec{r}\cdot\vec{q}/2}d^3\vec{r}\,, \tag{B11}$$

where A is the amplitude for emission of two photons by a nucleon, as discussed in Sec. 3.

*Work supported in part by the National Science Foundation, Grant No. GP-16565, and in part by the U. S. Atomic Energy Commission.

[1]R. J. Adler, B. T. Chertok, and H. C. Miller, Phys. Rev C 2, 69 (1970); *ibid.* 3, 2498(E) (1971).
[2]R. J. Adler, Phys. Rev. C 5, 615 (1972).
[3]H. P. Noyes, Nucl. Phys. 74, 508 (1965).
[4]N. Austern and E. Rost, Phys. Rev. 117, 1506 (1960).
[5]A. Cox, S. Wynchank, and C. Collie, Nucl. Phys. 74, 481 (1965).
[6]G. Breit and M. L. Rustgi, to be published. This contains a discussion of the capture of polarized n on polarized p and the role of the ^3S state in singly radiative capture.
[7]L. D. Landau, Nucl. Phys. 13, 181 (1959).
[8]R. E. Cutkosky, J. Math. Phys. 1, 429 (1960).
[9]J. D. Bjorken, Ph.D. thesis, Stanford University, 1959 (unpublished).
[10]J. D. Bjorken and S. D. Drell, *Relativistic Quantum Fields* (McGraw-Hill, New York, 1965), p. 235.
[11]M. Gell-Mann and M. Goldberger, Phys. Rev. 96, 1433 (1954).
[12]F. Low, Phys. Rev. 96, 1428 (1954).
[13]G. F. Chew, *S-Matrix Theory of Strong Interactions* (Benjamin, New York, 1961), p. 30.
[14]F. Gross, Phys. Rev. 140, B410 (1965).
[15]R. J. Adler, Ph.D. thesis, Stanford University, 1965 (unpublished), p. 106.
[16]F. Kaschluhn and K. Lewin, Nucl. Phys. 87, 73 (1966). An error in this paper is discussed in Ref. 1.
[17]R. J. Adler, Phys. Rev. 141, 1499 (1966).
[18]R. J. Adler, Phys. Rev. 169, 1192 (1968); 174, 2169(E) (1968).
[19]E. J. Squires, in *4th Scottish Universities Summer School*, edited by R. G. Moorehouse (Plenum, New York, 1965).
[20]L. I. Lapidus and Chou Kuang-Chao, Z. Eksperim. i Teor. Fiz. 39, 1286 (1960) [transl.: Soviet Phys.–JETP 12, 898 (1961)].
[21]I. J. Kalet, Phys. Rev. 176, 2135 (1968).
[22]N. K. Glendenning and G. Kramer, Phys. Rev. 126, 159 (1962).
[23]J. M. Blatt and V. F. Weisskopf, *Theoretical Nuclear Physics* (Wiley, New York, 1952), p. 63.
[24]B. Sakita and C. Goebel, Phys. Rev. 127, 1787 (1962).
[25]M. Skolnick, Phys. Rev. 136, B1493 (1964).
[26]B. Bosco, C. Ciocchetti, and A. Molinari, Nuovo Cimento 28, 1427 (1963).
[27]G. Stranahan, Phys. Rev. 135, B953 (1969).

PHYSICAL REVIEW C VOLUME 6, NUMBER 6 DECEMBER 1972

Regge Description of Optical-Model Scattering

T. Tamura and H. H. Wolter*
Center for Nuclear Studies, University of Texas,† Austin, Texas 78712

(Received 28 August 1972)

The analytic continuation of the S matrix into the complex angular momentum plane is performed exactly for the Woods-Saxon-type optical potentials, describing the elastic scattering of spinless but charged particles. The properties of this S matrix, such as the nature of the pole trajectories and the behavior of the background integral, are investigated for several specific cases. Based on these exact calculations, the validity of various approximations made in the Regge theory is assessed. It is found that approximations which retain only the pole terms are generally poor, being quite sensitive to the number and the positions of the poles and converging very slowly with an increasing number of poles. On the other hand, models using a simple analytic background term, in addition to one pole term, are found to reproduce the exact Regge amplitude quite accurately under favorable conditions. Suggestions are made for the possibility of extending this idea into a background-plus-several-pole model, when the background–one-pole model fails.

I. INTRODUCTION

Since the complex angular momentum approach was first introduced by Regge *et al.*,[1] it has been applied mostly to the relativistic rather than the nonrelativistic domain, in spite of the fact that various mathematical manipulations basic to the approach can be made rigorously only in the latter domain. The reason for this could have been that in nuclear and atomic physics, very little seems to be gained from this approach beyond what can be obtained by more conventional methods. However, interest has been revived recently, perhaps in relation to an increased investigation of heavy-ion-induced nuclear reactions. One finds that the scattering of such strongly absorbed particles can be described more easily and more uniquely in terms of a smooth cutoff S matrix, in contrast to optical-model fits which suffer from many discrete and continuous ambiguities.[2] More recently it was shown that the strong backward rise seen in heavy-ion scattering cross sections

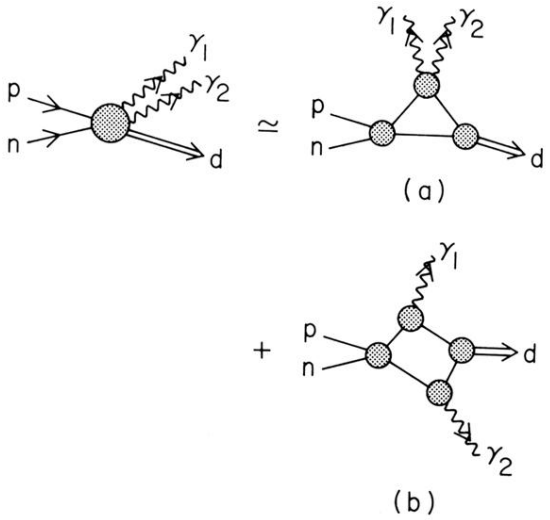

FIG. 1. The diagrams which represent the processes discussed in this paper. The first, (a), is the "Compton-like" process wherein one nucleon emits two real photons and enters the deuteron state with respect to the other nucleon, very much as in singly radiative *np* capture. The second, (b), is the "interference" process in which both nucleons emit a single photon.

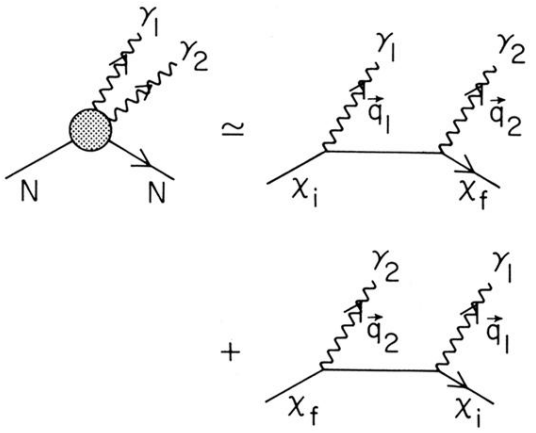

FIG. 2. The diagrammatic content of the generalized Compton amplitude used in this work. The photon γ_1 has three-momentum $\vec{q}_1$, energy ω_1, and polarization vector $\vec{\epsilon}_1$, and similarly for photon γ_2. The nucleon has an initial spin χ_i, final spin χ_f, charge e, and magnetic moment μ. We consider the nucleon to be initially at rest.

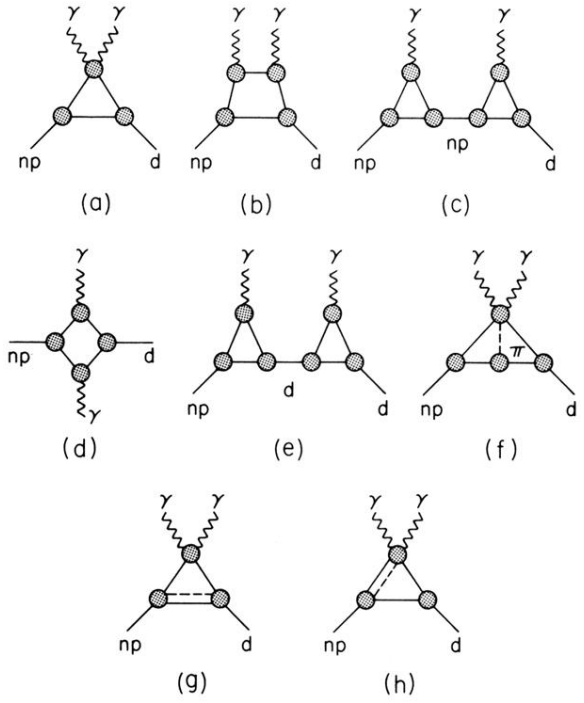

FIG. 4. Some diagrams whose singularity position is considered in Sec. 2 and Appendix A. Diagrams (a), (b), and (c) are implicitly contained in the diagram in Fig. 1(a), while (d) is the same as Fig. 1(b). These are singular at $q^2=4M\epsilon$. Other singularities are at: (e) $20M\epsilon$; (f) $4\mu^2$, where μ is the pion mass; (g) $16\mu M$; (h) $2M\mu$.